

The Study on Mg-Al Rich Epoxy Primer for Protection of Aluminum Alloy

Jianguo Wang, Yu Zuo*, Yuming Tang

School of Materials Science and Engineering, Beijing University of Chemical Technology, Beijing 100029, China

*E-mail: zuoy@mail.buct.edu.cn

Received: 29 May 2013 / Accepted: 19 June 2013 / Published: 1 August 2013

A Mg-Al rich epoxy primer was prepared by adding magnesium particles and aluminum particles to a epoxy coating. The Mg-Al rich primer with 20% Mg and 30% Al showed obviously better protection for 2A12 aluminum alloy than a Mg-rich primer with 50% Mg. By partly replacing Mg particles in Mg rich primer with Al particles, the cathodic protection of the Mg-Al rich primer with 20% Mg and 30% Al was not affected. The addition of Al particles decreased the distribution of Mg particles in the primer, which inhibited the intense galvanic function, decreased the formation of pores in the coating, and slowed down degradation of the coating. In addition, the relatively inert Al particles increased the barrier effect of the coating. As the results, the Mg-Al rich coating showed better protection and prolonged lifetime than the Mg-rich coating for 2A12 aluminum alloy.

Keywords: Aluminum alloy; Mg-Al rich primer; Cathodic protection; Barrier effect; Performance

1. INTRODUCTION

Aluminum alloys are widely used in automotive, aerospace and other industries because of their high strength and stiffness, combined with low density. However, Al alloys are sensitive to corrosion environments. For many applications it is necessary to improve the corrosion resistance of Al alloys [1-3]. Coating is one of the main corrosion control methods for metals and alloys in engineering applications. Among various coatings the zinc-rich primers (ZRPs) are frequently used for steels in which the active zinc particles dissolve preferentially and provide sacrificial protection to the steel substrate [4, 5]. Magnesium-rich primers were also reported for protection of Al alloys [6-17]. Nanna and Bierwagen [6] developed a Mg-based primer for the protection of aluminum structures and excellent performance for the Mg-rich primer coated aluminum panels in Prohesion testing was

observed. Battocchi and co-workers made further studies on the protection mechanism of aluminum substrate by Mg-rich primers [7-11]. The results showed that the Mg-rich primer provided protection to the Al substrate by a two-stage mechanism. In the first stage, corrosion of the aluminum substrate was prevented by cathodic protection provided by the Mg particles, whereas in the later stage the precipitation of a porous barrier layer of magnesium oxides was observed and corrosion was further inhibited by a barrier mechanism [7, 8]. The mechanism of cathodic protection of the aluminum substrates by Mg-rich coating was also investigated using localized techniques. It was shown that the cathodic protection provided by magnesium both prevented pit nucleation and inhibited the growth of the pre-existing pits on the aluminum substrates [9-13].

To provide sacrificial protection, the Mg particles in the primer have to be in electrical contact with the substrate and also with each other. Hence the Mg particles content must be near or above the Critical Pigment Volume Concentration (CPVC) for the coating. However, the large quantity of active Mg particles in the coatings may result in pores and flaws, and the intense galvanic effect between Mg particles and the Al substrate may lead to degradation of the resin. In this work, Mg particles in a Mg rich epoxy coating were partly replaced by aluminum particles, and the performance of the Mg-Al rich primer on 2A12 aluminum alloy was studied.

2. EXPERIMENTAL

2.1. Materials

2A12 aluminum alloy panels with the thickness of 3 mm were used as the substrate. The chemical composition was shown in Table 1.

Table 1. Nominal composition (wt.%) of 2A12 aluminum alloy

Cu	Mg	Mn	Fe	Si	Zn	Ni	Ti	Al
3.8~4.5	1.2~1.6	0.3~0.7	≤0.5	≤0.5	≤0.3	≤0.1	0.15	Bal.

The epoxy paint used in this study was a two component commercial epoxy (KFH-01, from Shijiazhuang Golden Fish Paint Company, China). The silane coupling agent, γ -glycidoxy propyl trimethoxy silane (γ -GPS), was obtained from Beijing Antepuna Trade Co., Ltd, China. The pure Mg particles (99.9%), with the average size of 10-20 μm , were prepared by Beijing Nachen Science and Technology Co., Ltd. The pure Al particles (99.9%), with the average size of 17 μm , were prepared by Beijing Haoyunjinneng Science and Technology Co., Ltd.

2.2. Sample preparation

The aluminum alloy was cut into the size of 50 × 50 × 3 mm, then the samples were ground using SiC abrasive papers up to 240 grit, washed in distilled water and acetone in turn, and dried in air.

The Mg-rich primer was prepared by adding different contents of pure magnesium particles and aluminum particles into the epoxy paint (with respect to the dry paint film weight), as shown in Table 2. γ -GPS coupling agent (1% w/w with respect to the pigment weight) was added in the primer as dispersing agent. A high speed agitation equipment was employed for dispersion of the pigments. After dispersion for 10 min, the curing agent polyamide was added to the primer. The weight ratio of polyamide and epoxy was 3:10. Then the primer was applied on the aluminum alloy samples by manual brushing. After coating, the samples were cured for a week at room temperature. The thickness of the dry primer was about $85 \pm 5 \mu\text{m}$ which was measured with a digital thickness gauge TT230.

Table 2. The pigment contents in the Mg-Al rich epoxy coatings (wt.%)

Sample	Mg particles	Al particles	Abbreviation
A	50	0	50Mg
B	40	10	40Mg10Al
C	30	20	30Mg20Al
D	20	30	20Mg30Al
E	10	40	10Mg40Al
F	0	50	50Al

2.3. Machu test

This test is designed to evaluate corrosion performance of painted metals. The painted metal panels were cross-scribed on the surface prior to the test, then were immersed in a solution of 5% NaCl + 10% H_2O_2 + 10 mL/L acetic acid at 37 °C for 1 day. In the next day, again 10% H_2O_2 was added in the original solution. After 2 days of immersion, corrosion phenomena along the scratches were observed.

2.4. The scratch testing

Cross scratch tests were carried out for the coated aluminum alloy samples to examine the corrosion resistance of the coatings. The edges of the samples were sealed with HY-914 resin. A cross scratch, 2.5 cm long and deep to the matrix, was made on the coated sample surface with a razor blade. Then the samples were immersed in 3 wt.% NaCl solution (pH=7, room temperature) and corrosion phenomena along the scratches were observed.

2.5. Electrochemical measurements

EIS measurements were carried out in 3 wt.% NaCl solution with a PARSTAT 2273 system, over the frequency range from 100 kHz to 0.01 Hz at open circuit potential, with a 10 mV potential perturbation. The exposed working area was 10 cm^2 . A three-electrode arrangement was used,

consisting of a saturated calomel electrode (SCE) as reference electrode, a platinum electrode as counter electrode, and the coated sample as the working electrode. Fitting of the impedance spectra was made using ZSimpWin software.

2.6. SEM observation

A Hitachi S4700 field emission scanning electron microscope (SEM) was used to characterize the morphology of the coating. The operating potential of the field emission source was 20 kV. The samples were coated with gold to preclude the charging effect during measurement.

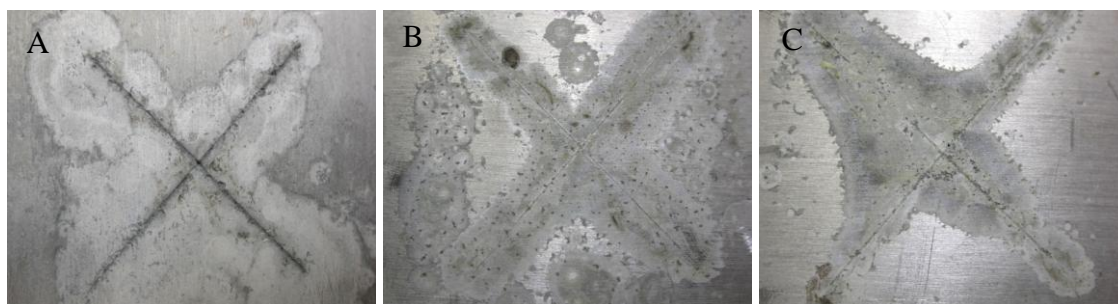
3. RESULTS AND DISCUSSION

3.1. Machu test

Machu test results for the scratched coating samples after coating removed are shown in Fig. 1. For sample A, corrosion was slight which may be due to the effect of Mg particles, but the corroded area extended most of the field. For sample B and sample C, obvious corrosion damages are also observed around the scratches. For sample E and sample F which contained only 10% Mg or less, the substrate was corroded severely. Among the Mg-Al rich coatings sample D (20Mg30Al) showed relatively the best protection, while the coatings with more or less than 30% w/w Al particles behaved worse. The addition of Al particles decreased the content of Mg in the primer, slowed up the intense galvanic reaction, and increased the barrier effect of the coating to some extent. However, as the content of Al particles was above 30% w/w in the coating, the cathodic protection provided by Mg particles was inhibited.

3.3. The scratch testing results

Cross scratches were made on the coated samples. Then the samples were immersed in 3 wt.% NaCl solution. Fig. 2 shows the surface morphology of the samples after 150 days of immersion. For samples A, B and C, corrosion products were obviously seen on the surface along the scratches. For sample E and F, slight bulges may be observed at the edge of the scratches.



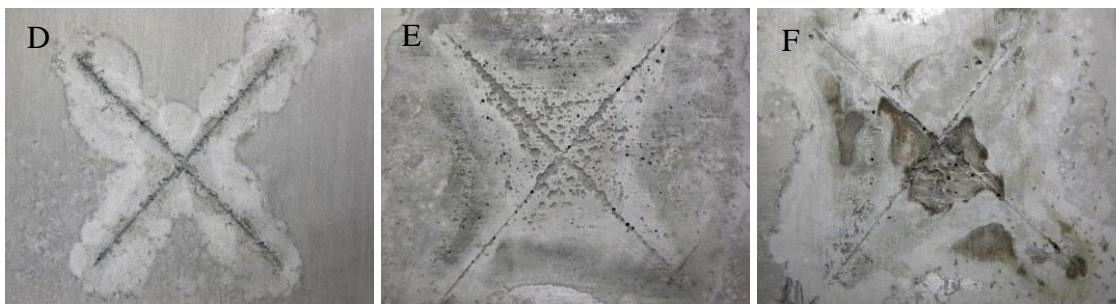


Figure 1. Machu testing results of scratched coating samples after coating removed: A) 50Mg; B) 40Mg10Al; C) 30Mg20Al; D) 20Mg30Al; E) 10Mg40Al; F) 50Al

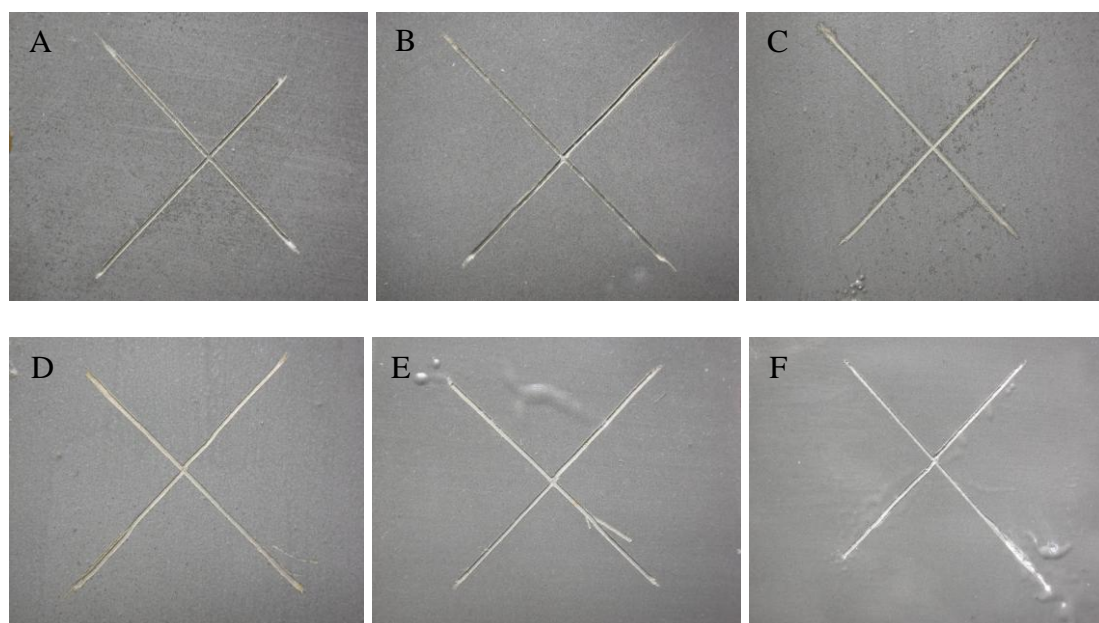


Figure 2. Surface morphology of the scratched coating samples after immersion in 3%NaCl solution for 150 days: A) 50Mg; B) 40Mg10Al; C) 30Mg20Al; D) 20Mg30Al; E)10Mg40Al; F)50Al

Among the 6 samples, sample D provided the best protection to the 2A12 alloy substrate. This result is consistent with above Machu test result. The addition of Al particles decreased the distribution of Mg particles in the primer surface, leading to less corrosion products of magnesium in the coating.

3.4 The electrochemical studies

The open circuit potential (OCP) for the 2A12 aluminum alloy samples with coatings was monitored as a function of time. Fig. 3 shows the OCP variations of the Mg-Al rich primer coated 2A12 alloy samples in 3% NaCl solution. In the beginning stage, the OCP for all the samples with different Mg-Al ratios was below the corrosion potential of bare 2A12 alloy which was about $-0.65 V_{SCE}$, indicating that cathodic protection was provided by all the primers. It is interesting to note that even for coating F, in which there were only aluminum particles, the OCP of the coating/alloy system

was also below the corrosion potential of bare 2A12 alloy. This may be attributed to the effect of the alloying elements such as Cu in 2A12 alloy, which resulted in an increased potential for the 2A12 alloy substrate than that of the pure aluminum particles in the coating. After immersion for about 100 days, the OCP of sample F moved above $-0.65 V_{SCE}$. However, for the samples of 30Mg20Al, 20Mg30Al and 10Mg40Al, the OCP values remained relatively stable below $-0.65 V_{SCE}$ during 280 days of immersion. This result confirms that when part of Mg particles in the coating is replaced by Al particles, the cathodic protection of the coating is not influenced.

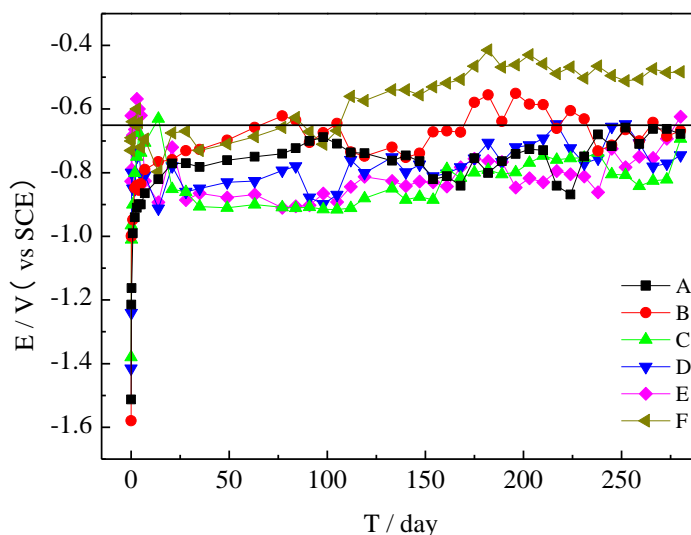


Figure 3. Open circuit potential variations of the Mg-Al primer coated 2A12 samples in 3% NaCl solution: A) 50Mg; B) 40Mg10Al; C) 30Mg20Al; D) 20Mg30Al; E) 10Mg40Al; F) 50Al

Fig. 4 shows the measured low frequency impedance modulus $|Z|$ values of the coated samples versus the exposure time in 3% NaCl solution. For all the samples, the $|Z|$ values decreased gradually during the initial immersion time as a result of the electrolyte permeation into the coating and the activation of the Mg particles [19]. Then, the $|Z|$ values increased gradually. This phenomenon may be attributed to precipitation of the corrosion products of magnesium in the primer, which provides a barrier protection to some degree [20]. As the immersion time prolonging, the $|Z|$ values of all samples decreased slowly, suggesting the increase of pores or capillary channels in the coatings [21, 22]. The $|Z|$ value of the sample with 50Al coating is the highest among the six tested samples. Compared with magnesium particles, aluminum particles are more inertial, which is beneficial to the barrier behavior of the coating [18]. However, after 200 days of immersion, the $|Z|$ value of the sample with 50Al coating and 10Mg40Al coating decreased notably, suggesting weakening of the barrier protection of those coatings. Therefore, above results show that for the Mg-Al rich coatings, higher Mg content is beneficial to the cathodic protection effect of the coating for the substrate, while higher Al content is beneficial to the barrier effect. As the consequence, an appropriate Mg/Al ratio is in favor of both the cathodic protection and the barrier effects. The results in Fig. 4 also indicate that the coating with 20Mg30Al showed relatively the best protection: After 160 days of immersion, the $|Z|$ value of the sample 20Mg30Al became larger than that of sample 50Mg, and remained stable until the end of the

test (280 days). This indicates that the performance of the Mg-rich primer was improved by the addition of certain amount of Al particles.

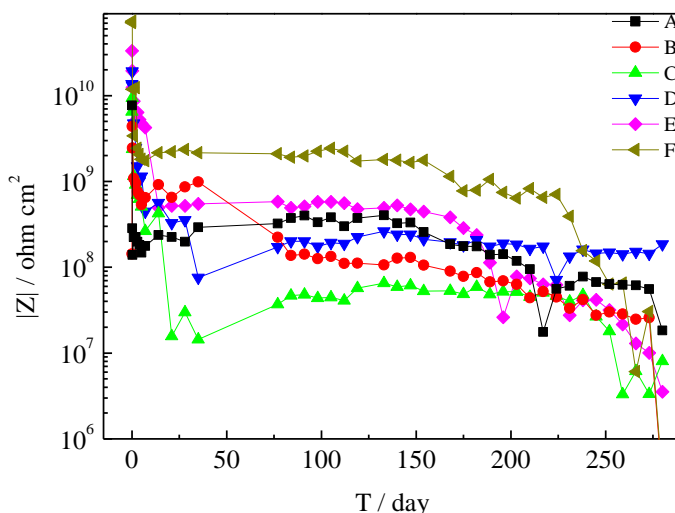
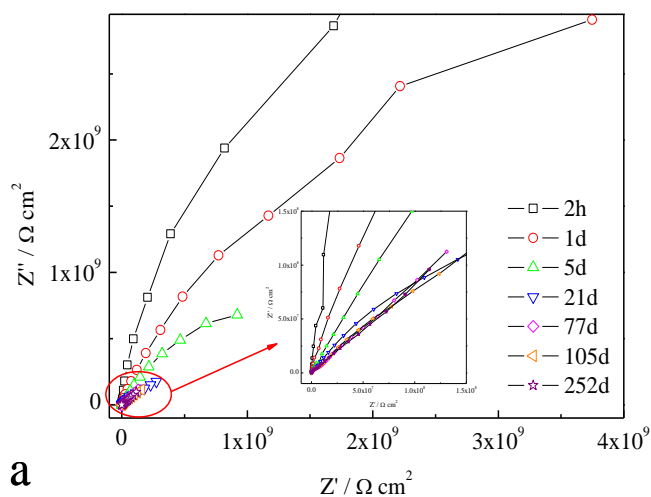


Figure 4. $|Z|$ modulus at 0.01Hz for Mg-Al primer coated 2A12 samples in 3% NaCl solution: A) 50Mg; B) 40Mg10Al; C) 30Mg20Al; D) 20Mg30Al; E) 10Mg40Al; F) 50Al

3.5 EIS study on the sample with 20Mg30Al coating

The EIS spectra for the sample with the 20Mg30Al coating were measured to understand the coating performance during immersion test. Fig. 5 shows the results. During initial immersion (1-24 h), the Nyquist plot showed a high impedance semi-circle, and the impedance modulus was higher than $10^{10} \Omega \text{ cm}^2$ at the low frequency end (0.01 Hz), which reflects a classical barrier-type coating behavior. With the increase of immersion time, the diameter of the semi-circle decreased showing the permeation of electrolyte into the coating [7, 21-23].



a

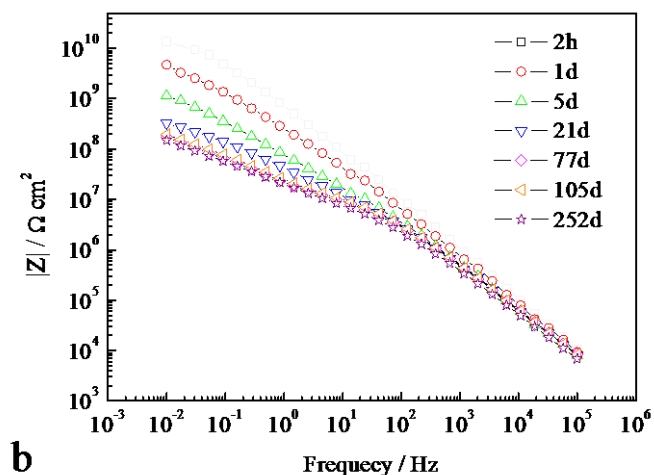


Figure 5. Impedance spectra of 2A12 alloy with the 20Mg30Al primer after different immersion times in 3 wt.% NaCl solution: (a) Nyquist plots, (b) Bode plots.

From 21 d to 205 d, there were no significant changes in the impedance spectra and the low frequency $|Z|$ value decreased slowly, indicating that the protective property of the primer maintained stable without obvious deterioration.

The EIS spectra can be fitted well using the equivalent circuits (EEC) shown in Fig. 6. To obtain more precise results, the capacitive responses were fitted by constant phase elements, Q , whose impedance is defined as

$$Z_Q = \frac{1}{Y_0(j2\pi f)^n}$$

in which Y_0 is the CPE constant, $j = \sqrt{-1}$, f is the frequency (Hz), the exponent n is equal to $\alpha/(\pi/2)$, and α the phase angle of the CPE (radians). During initial immersion (1–8 h), the coating sample showed classical barrier-type behavior. Therefore, the EIS spectra can be fitted well using a simple equivalent electrical circuit (EEC) as shown in Fig. 6a which is composed of the coating capacitance Q_c in parallel to the coating resistance R_c [7, 8, 11]. After 24 h of immersion, model A does not fit the EIS data well due to the accumulation of corrosion products at the magnesium particles/electrolyte interface. The EIS spectra could be explained in terms of model B (Fig. 6b), in which R_{ct} is the charge-transfer resistance of the magnesium particles and Q_{dl} is the double-layer capacitance at the magnesium particles/electrolyte interface. The diffusion behavior caused by the presence of the corrosion products of magnesium particles is not an ideal Warburg impedance. The impedance response is probably associated with finite-layer diffusion. Then the capacitance Q_{diff} in parallel to resistance R_{diff} can be noted as Z_{diff} , which could be correlated to diffusion processes caused by presence of the corrosion products of magnesium particles [7, 8, 11]. After 91 d of immersion, the EIS spectra can be fitted well using the EEC shown in Fig. 6c. In model C, Q_c is the coating capacitance, R_c is the coating resistance, R_{ct} is the charge-transfer resistance of the magnesium particles, Q_{dl} is the double-layer capacitance at the magnesium particles/electrolyte interface, C_{sf} is the

film capacitance of the corrosion products on the alloy substrate and R_{sf} is the resistance of the corrosion products film on the alloy substrate [21-22]. The fitting results are shown in Fig. 7.

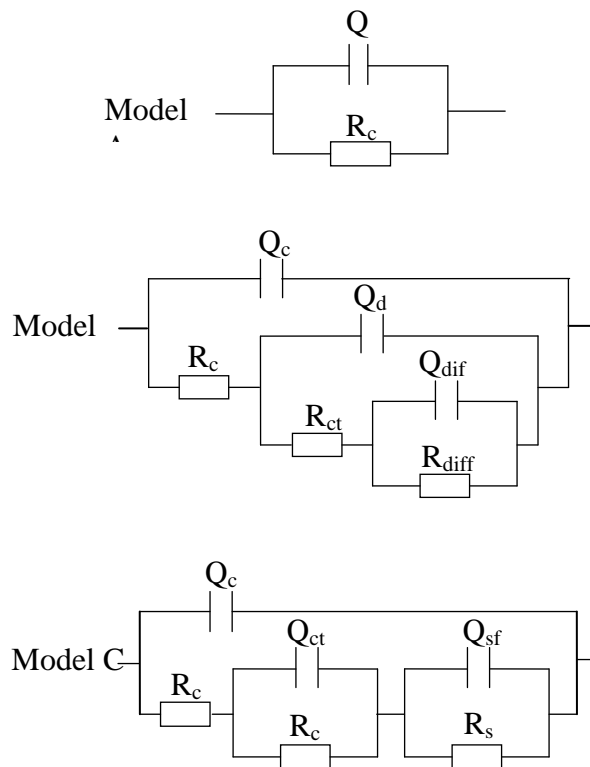


Figure 6. The equivalent electrical circuits for EIS spectra of the Mg-Al primer coated samples after different immersion time in 3%NaCl solution

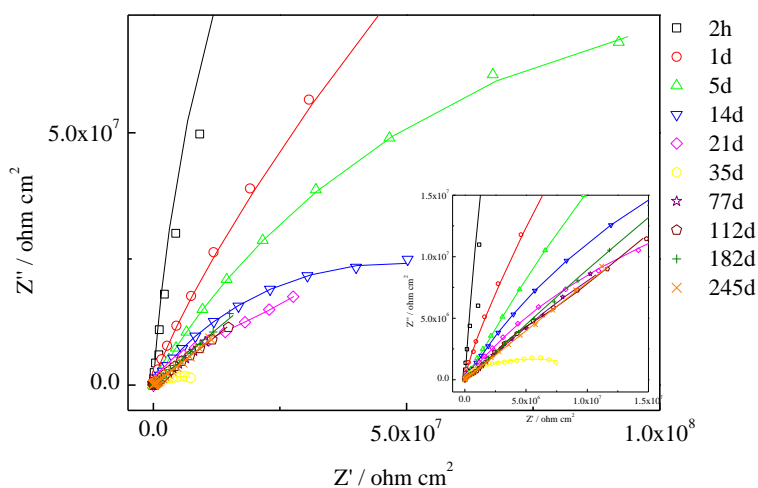


Figure 7. Fitting of EIS spectra for 20Mg30Al primer coated sample after different immersion time in 3%NaCl solution: dot: experimental data, line: fitting results

Fig. 8 shows the variations of the obtained impedance parameters from EIS results for 20Mg30Al and 50Mg coatings as the function of immersion time. The coating resistance R_c is a

measure of the porosity and the deterioration of coatings [27]. During first 24 h of immersion, the R_c values of both coatings exhibited notable decrease (Fig. 8a) because of penetration of the electrolyte and the increase of pores or capillary channels in the coating [19]. Then, the R_c values increased gradually. This phenomenon may be attributed to precipitation of corrosion products of magnesium in the primer, which provides the barrier protection to some degree [20], corresponding to the variation of the low frequency impedance modulus $|Z|$. During the immersion test the R_c value for the sample with 20Mg30Al coating was higher than that of the sample with 50Mg coating by approximately two orders of magnitude, suggesting better barrier properties. This result also confirms that the addition of Al particles prolonged lifetime of the primer on 2A12 alloy.

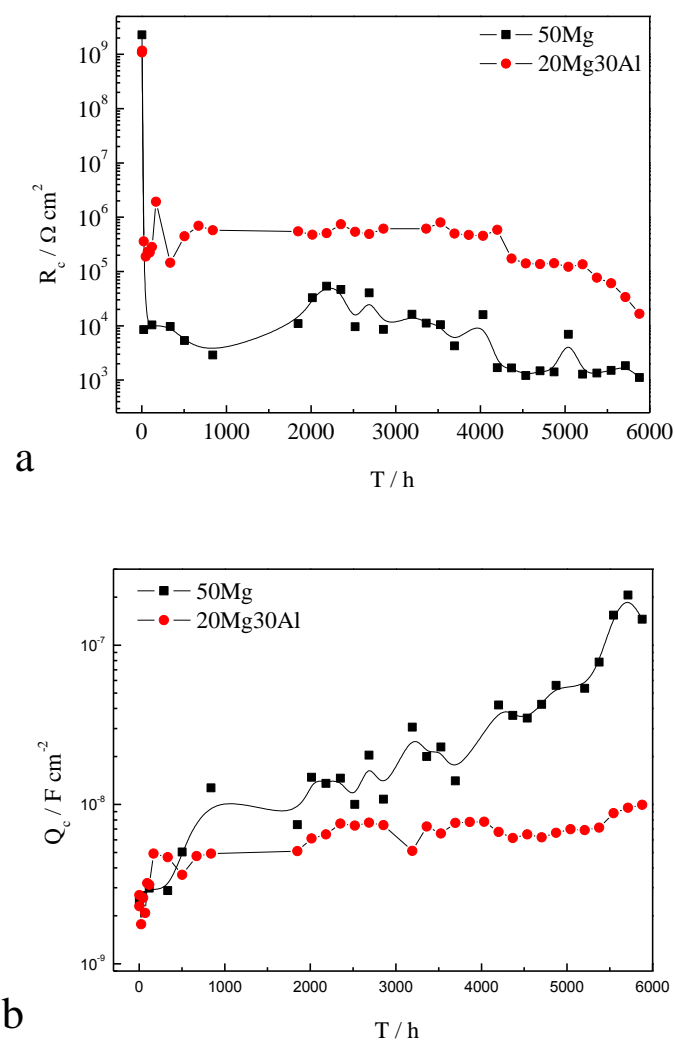


Figure 8. The variations of the impedance parameters for 2A12 alloy with 50Mg primer or with 20Mg30Al primer with immersion time, (a) R_c , and (b) Q_c

The coating capacitance Q_c reflects the electrolytic penetration in coating. During first 200 h immersion, the Q_c values of both coatings increased rapidly (Fig. 8b) because of the electrolyte penetration. After the initial immersion, the Q_c value of the sample with 50Mg coating continued to increase notably, while that of the sample with 20Mg30A coating remained almost constant until the

end of the test. This may be attributed to the relatively inertial Al particles which partly replaced Mg particles, leading to less dissolved particles and decreased porosity [24-26]. Meanwhile, the addition of the relatively inertial Al particles also may inhibit the penetration of electrolyte [23].

R_{ct} is an indication of the electrochemical reaction tendency of the magnesium particles [7, 21]. Fig. 9a shows the variation of R_{ct} as a function of immersion time. As the immersion time prolonged, the R_{ct} value of the sample with 50Mg coating tended to decrease, indicating the activation of Mg particles. However, a slight increase occurred after 2500 h of immersion, which may be because that the corrosion products of the magnesium particles accumulated and restricted the active zones on the surface of magnesium particles. On the other hand, the sample with 20Mg30Al coating showed higher R_{ct} value during the whole immersion.

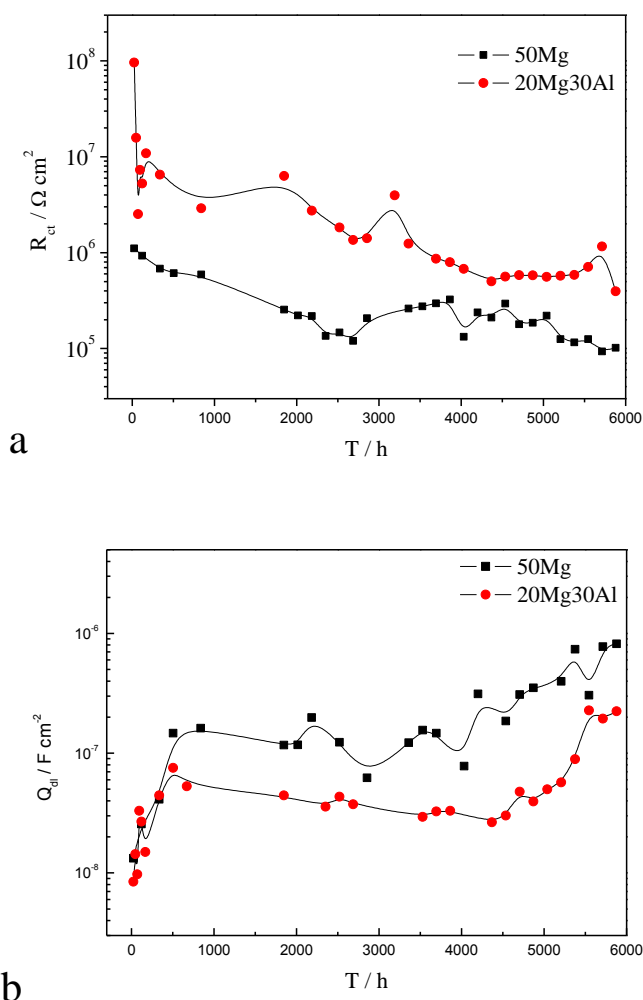


Figure 9. The variations of the impedance parameters for 2A12 alloy with 50Mg primer or with 20Mg30Al primer with immersion time, (a) R_{ct} , and (b) Q_{dl}

Fig. 9b shows the variation of Q_{dl} as a function of immersion time. Q_{dl} is an indication of the active area at the magnesium particles/electrolyte interface. During first 500 h immersion, the Q_{dl} values of both coatings increased rapidly (Fig. 9b) because of penetration of the electrolyte. As the

result the number of Mg particles exposed to electrolyte increased and the active area increased. Then, the Q_{dl} values of both coatings decreased slowly, suggesting the accumulation of the corrosion products on the surface of Mg particles. After 4500 h of immersion, the Q_{dl} values increased again, indicating degradation of the coating. The Q_{dl} value of the sample with 20Mg30Al coating remained smaller than that of the sample with 50Mg coating during the test, again confirming the improved protection by the addition of Al particles in the coating.

Fig. 10 shows surface morphology of the 50Mg coating and the 20Mg30Al coating after 84 days of immersion in 3% NaCl solution. Many notable pores, produced by the dissolution of Mg particles near the surface, exist on the surface of the 50Mg sample, while the surface of 20Mg30Al sample is smooth without pores.

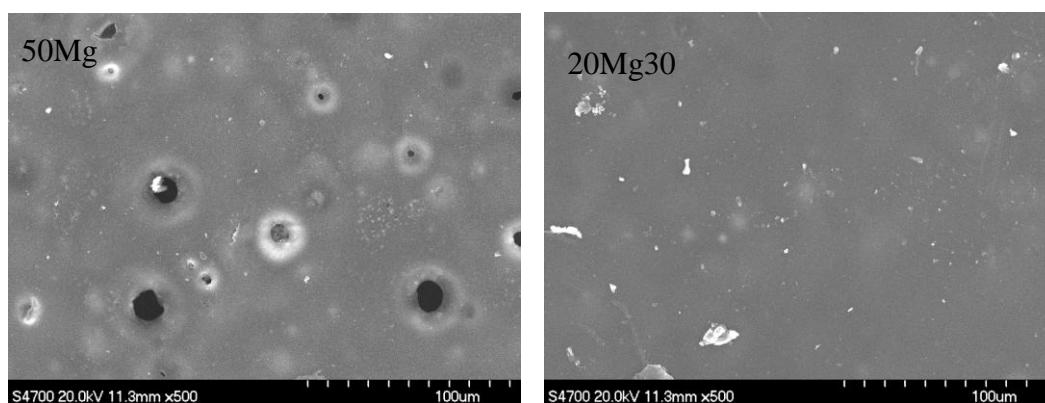


Figure 10. Surface morphology of the 50Mg primer and the 20Mg30Al primer after 84 d of immersion

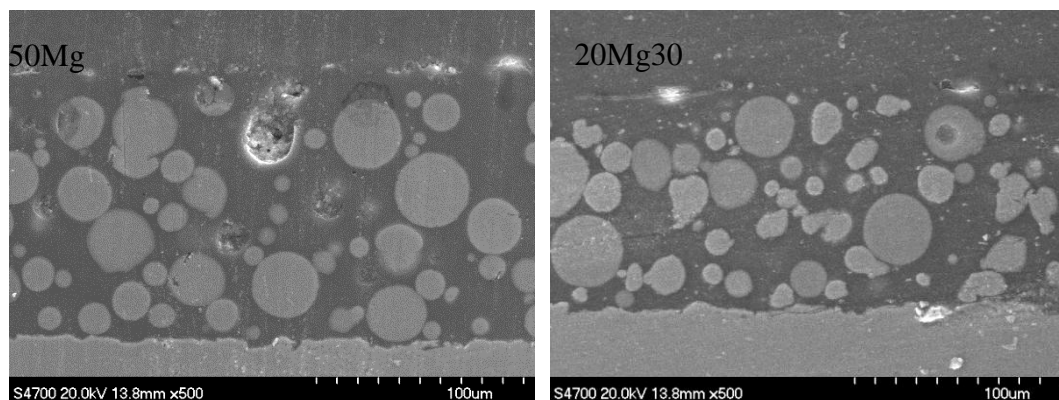


Figure 11. The cross-section morphology of the 50Mg primer and the 20Mg30Al primer after 84 d of immersion

There are two possible reasons resulting in this difference. Firstly, the addition of Al particles decreases the distribution of Mg particles in the coating. Secondly, the Al particles inhibits the intense galvanic function, slows down the degradation of coating [18]. This result indicates that the addition of Al particles prolonged the lifetime of the Mg-rich primer on 2A12 alloy, corresponding to previous EIS results.

Fig. 11 shows cross-section of the 50Mg coating and the 20Mg30Al coating after 84 days of immersion in 3% NaCl solution. For the 50Mg sample, some Mg particles near the top of coating have dissolved, which may result in the appearance of pores on the coating surface as shown in Fig 10a. For the 20Mg30Al sample, the Mg particles and the Al particles can not be distinguished obviously in the coating (Fig.11b). However, the dissolution of both particles was not found.

It has been defined that the Mg-rich primer provides good protection to Al alloy [5-11]. Previous study on zinc-rich primers [28] showed that the performance of the primer is not related to the content of zinc. Only 25% zinc in the primer provided the cathodic protection. Therefore, for Mg-rich primer, not all the Mg particles are necessary for the galvanic protection. Through the results of OCP, it is seen that the cathodic protection of the coating was not affect by certain amounts of addition of Al particles. In the same time, the addition of Al particles decreased the distribution of Mg particles in the primer, which inhibited the intense galvanic function, decreased the formation of pores in the coating, and slowed down the degradation of coating [18]. On the other hand, the relatively inert Al particles increased the barrier effect of the coating. As the results, the Mg-Al rich coating showed better protection and prolonged lifetime than the Mg-rich coating for 2A12 aluminum alloy.

4. CONCLUSIONS

(1) Al particle was added in Mg-rich epoxy coating to improve the protective behavior of the Mg-rich primer on 2A12 aluminum alloy. The Mg-Al rich primer with 20% Mg and 30% Al showed obviously better protection for 2A12 alloy than a Mg-rich primer with 50% Mg.

(2) By partly replacing Mg particles in Mg rich primer with Al particles, the cathodic protection effect of the Mg-Al rich primer with 20% Mg and 30% Al was not affected.

(3) The effects of Al particle in the Mg-Al rich primer are suggested as follows: The addition of Al particles decreases the distribution of Mg particles in the primer, which inhibits the intense galvanic function, decreases the formation of pores in the coating, and slows down degradation of the coating. In addition, the relatively inert Al particles increased the barrier effect of the coating.

References

1. Y. Liu, G.Z. Meng, Y.F. Cheng, *Electrochim. Acta*, 54 (2009) 4155
2. F. Girardi, F. Graziola, P. Aldighieri, L. Fedrizzi, S. Gross, R.D. Maggio, *Prog. Org. Coat.*, 62 (2008) 376
3. Z.Z. Han, Y. Zuo, P.F. Ju, Y.M. Tang, X.H. Zhao, J.L. Tang, *Sur. Coat. Technol.*, 206 (2012) 3264
4. O. Ø. Knudsen, U. Steinsmo, M. Bjordal, *Prog. Org. Coat.*, 54 (2005) 224
5. H. Marchebois, C. Savall, J. Bernard, S. Touzain, *Electrochim. Acta*, 49 (2004) 2945
6. M.E. Nanna, G.P. Bierwagen, *JCT research*, 1 (2004) 69.
7. D. Battocchi, A.M. Simões, D.E. Tallman, G.P. Bierwagen, *Corros. Sci.*, 48 (2006) 1292
8. D. Battocchi, A.M. Simões, D.E. Tallman, G.P. Bierwagen, *Corros. Sci.*, 48 (2006) 2226
9. A.M. Simões, D. Battocchi, D.E. Tallman, G.P. Bierwagen, *Corros. Sci.*, 49 (2007) 3838
10. G. Bierwagen, D. Battocchi, A. Simões, A. Stamness, D. Tallman, *Prog. Org. Coat.*, 59 (2007) 172

11. A. Simões, D. Battocchi, D. Tallman, G. Bierwagen, *Prog. Org. Coat.*, 63 (2008) 260
12. D.L. Schulz, R.A. Sailer, C. Braun, *Prog. Org. Coat.*, 63 (2008) 149
13. D.H. Wang, D. Battocchi, K.N. Allahar, S. Balvyshev, G.P. Bierwagen, *Corros. Sci.*, 52 (2010) 441
14. G. Bierwagen, R. Brown, D. Battocchi, S. Hayes, *Prog. Org. Coat.*, 67 (2010) 195
15. H. Xu, D. Battocchi, D.E. Tallman, G.P. Bierwagen, *Corros.*, 65 (2009) 318
16. L.M. Liu, R.Z. Xu, G. Song, *Sur. Coat. Technol.*, 205 (2010) 332
17. M.C. Yan, V.J. Gelling, B.R. Hinderliter, D. Battocchi, D.E. Tallman, G.P. Bierwagen, *Corros. Sci.*, 52 (2010) 2636.
18. A. Gergely, É. Pfeifer, I. Bertóti, T. Török, E. Kálmán, *Corros. Sci.*, 53 (2011) 3486
19. C.M. Abreu, M. Izquierw, M. Keddám, X.R. Nvoas, H. Takenout, *Electrochim. Acta*, 41 (1996) 2405
20. A. Meroufel, S. Touzain, *Prog. Org. Coat.*, 59 (2007) 197
21. X.Y. Lu, Y. Zuo, X.H. Zhao, Y.M. Tang, X.G. Feng, *Corros. Sci.*, 53 (2011) 153
22. X.Y. Lu, Y. Zuo, X.H. Zhao, Y.M. Tang, *Corros. Sci.*, 60 (2012) 165
23. Y.P. Wang, X.H. Zhao, X.Y. Lu, Y. Zuo, *Acta Physico-chimica Sinica*, 28 (2012) 407
24. H. Marchebois, S. Touzain, S. Joiret, J. Bernard, C. Savall, *Prog. Org. Coat.*, 45 (2002) 415
25. H. Marchebois, C. Savall, J. Bernard, S. Touzain, *Electrochim. Acta*, 49 (2004) 2945
26. H. Marchebois, M. Keddám, C. Savall, J. Bernard, S. Touzain, *Electrochim. Acta*, 49 (2004) 1719
27. J.M. Hu, J.Q. Zhang, C.N. Cao, *Prog. Org. Coat.*, 46 (2003) 273
28. Z.N. Yu, *Corrosion Resistant Paint and Finishing*, Chemical Industry Press, Beijing (2002)